JCIM JOURNAL OF CHEMICAL INFORMATION AND MODELING

pubs.acs.org/jcim Letter

Evidence for Epibatidine Binding to the Desensitization Gate in α7 nAChR from Molecular Dynamics Simulations and Cryo-EM

Jesko Kaiser, Christoph G. W. Gertzen, Daniel Mann, Carsten Sachse, and Holger Gohlke*

Cite This: J. Chem. Inf. Model. 2026, 66, 1337−1341 Read Online

ACCESS | Metrics & More | Article Recommendations | Supporting Information

ABSTRACT: The homopentameric α7-nicotinic acetylcholine receptor (nAChR) is a ligand-gated ion channel widely expressed in the human nervous system and susceptible to allosteric modulation. A recent cryo-EM structure (EMD 22983; PDB ID 7KOX) revealed unassigned Coulomb density. Unbiased molecular dynamics simulations of buffer components around α7-nAChR show that (±)-epibatidine can occupy not only the orthosteric site but also the pore near the desensitization gate, consistent with the unmodeled Coulomb density and expanding the receptor's pocketome.

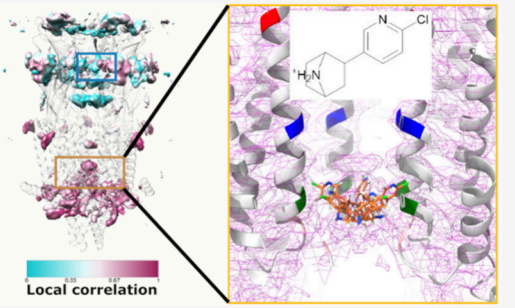

The α7 nicotinic acetylcholine receptor (nAChR) is a pentameric ligand-gated ion channel that plays a crucial role in physiological processes in the human brain.[1] During the activation cycle, the receptor can adopt three distinct states. After the binding of competitive agonists, the receptor undergoes structural rearrangements from an inactive state to an active one with an open pore conformation, enabling ions to pass through the receptor. However, after overstimulation, nAChRs can adopt a desensitized state, featuring a funnel-shaped pore with a constriction site at the position −1′, resulting in a nonfunctional, nonactivatable state (Figure S1).[2−5] Mechanisms leading to desensitization of the receptor remain incompletely understood. Several allosteric modulators have been described to impact the activation and desensitization of the receptor.[6−11] Recently, the first cryo-EM structures of the α7-nAChR in all three states (inactive, active, desensitized) have been resolved (PDB IDs: 7KOO, 7KOX, 7KOQ), revealing further insights into differences between the states.[4] Strikingly, the corresponding cryo-EM map (EMD 22983) resolved at a nominal resolution of 2.7 Å of the active state shows unmodeled Coulomb density in two regions of the receptor pore (Figure S2A-D) suggesting binding of additional molecules in these regions. For other receptors, such as G protein-coupled receptors, or compounds in other pentameric ligand-gated ion channels, such as benzodiazepines, recent publications revealed additional potential binding sites indicating that the pocketome of most receptors might not have been completely identified.[12−14] Thus, to shed light on which molecules might bind in the regions of unmodeled cryo-EM density in α7-nAChR, we performed 12 replicas of 3 μs long unbiased molecular dynamics (MD) simulations of free ligand diffusion.[15,16] In each replica, molecules present in the experimental buffers used to obtain the cryo-EM structures, Ca^{2+}, (±)-epibatidine, PNU-120596, Na^+, Cl^-, and Tris, were placed at random positions in the water phase of the simulation box around α7-nAChR in the active state embedded in a membrane at concentrations of ∼4 mM except 150 mM for NaCl and 20 mM for Tris, as used in experiments (see also Materials and Methods in the SI).

During the simulations, the receptor and membrane remained structurally invariant (Figures S3, S4). To compare the occupancy density of the molecules observed in the MD simulations with the unmodeled cryo-EM densities, we applied a C5 symmetry to the occupancy densities (Figure S5), as done for the experimental cryo-EM maps.[4] In the cryo-EM-derived atomic models of α7-nAChR in all three states (PDB IDs: 7KOX, 7KOO, 7KOQ[4]), a binding site for calcium between E44 and E172 was resolved. This binding site was identified in our simulations, too, acting as a positive control (Figure S6; for RMSD values compared to the binding mode in the cryo-EM structure, see Figure S7). However, no binding site for PNU-120596 was resolved in these structures. In our MD simulations, we observed binding of PNU-120596 in the pore just a few Å away from its reported intersubunit transmembrane pocket in PDB ID: 8V82[17], ∼18 Å above the desensitization gate. We also observed that sodium binds to the binding site of calcium (Figure S8), indicating that this region attracts positively charged moieties. This is in line with the assumption that the double positively charged positive

Received: September 30, 2025
Revised: January 15, 2026
Accepted: January 16, 2026
Published: January 27, 2026

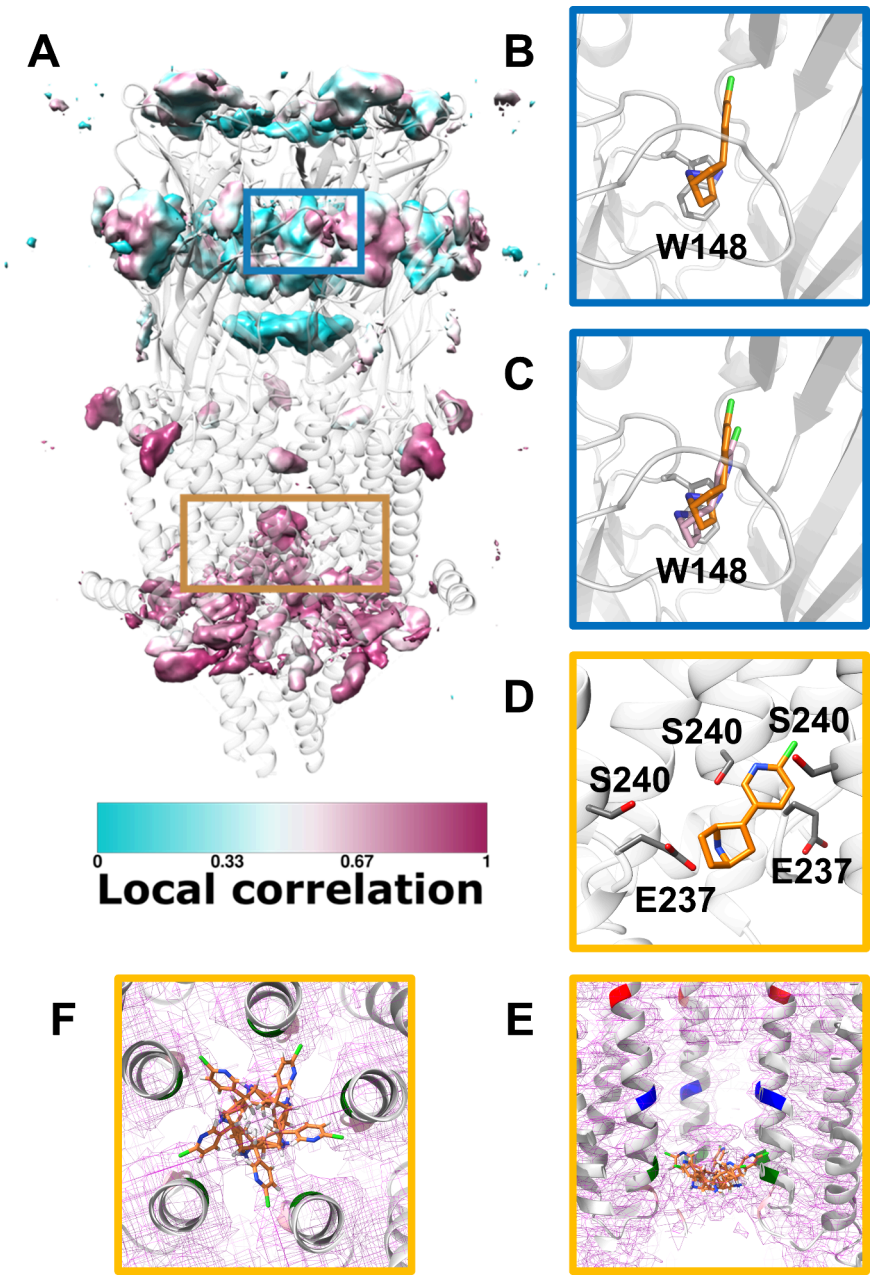

Figure 1. Local correlation map between the occupancy density of epibatidine during MD simulations and the cryo-EM map (EMD 22983[4]). (A) The occupancy density (density threshold 0.05) color coded with local correlation to the cryo-EM Coulomb density is mapped on the active structural model of the human α7-nAChR (PDB ID: 7KOX[4]). Red colors indicate a high local correlation and blue colors a low local correlation. Regions of high local correlation are highlighted by boxes; the colors indicate the close-up of each binding site in panels B−F, respectively. (B) Exemplary binding mode of epibatidine (orange) in the orthosteric binding site. For all epibatidine binding modes at the end of the MD simulations see Figure S10. (C) Comparison of the epibatidine binding mode observed in MD simulations (orange) to the epibatidine binding mode in the cryo-EM structure of α7-nAChR (PDB ID: 7KOX[4]) (purple) (for alignment details see Materials and Methods in the SI). (D) Exemplary epibatidine (orange) binding mode at the desensitization gate. For all epibatidine binding modes at the end of the MD simulations, see Figure S12. (E) Exemplary epibatidine (orange) binding mode from panel D shown in 5-fold symmetry in the cryo-EM Coulomb density at threshold 0.005 (pink). All symmetrized ligands are covered by Coulomb density, although only one ligand could bind at a time due to steric reasons. The inactivation gate (L247, position 9′) is colored in blue. S240 (position 2′), used to characterize binding at the desensitization gate (see Materials and Methods in the SI and panel D), is colored in green. A257, used to characterize binding in the extracellular end of the transmembrane domain (see see Materials and Methods in the SI), is colored in red. (F) Top-down view of panel E.

allosteric modulator MB327 binds to the same binding site.[18] To identify further potential binding sites, we focused on regions displaying a high local correlation between occupancy densities observed during MD simulations and densities of the cryo-EM map of the human α7-nAChR (EMD 22983[4]) at a false discovery rate of 1% (see Materials and Methods in the SI) (Figure 1A, Figure S9). A high local correlation for epibatidine is found in the orthosteric binding site, which provided another positive control (Figure 1A−C). During the free ligand diffusion MD simulations, we observed 13 binding events in the orthosteric binding site (Table S1), where a binding event was recorded if the distance of ligand heavy

https://doi.org/10.1021/acs.jcim.5c02384
J. Chem. Inf. Model. 2026, 66, 1337−1341

atoms to W148, an amino acid central in the binding site, was below 5 Å, as used before to characterize binding in nAChRs,[18−20] for at least 100 consecutive ns. The ligand then remains within the binding site until the end of the MD simulations in 11 cases (Figure S10; for RMSD values compared to the binding mode in the cryo-EM structure, see Figure S11). Furthermore, we observed a high local correlation between epibatidine binding within the pore of α7-nAChR and the unmodeled Coulomb density there in the cryo-EM map (PDB ID: 7KOX, EMD 22983[4]). Particularly interesting is the high local correlation at the desensitization gate (Figure 1A), which has been suggested to hinder ion transfer in the desensitized state of the receptor.[5] We observed six binding events at the desensitization gate (Figure 1D, Table S2). However, in contrast to the orthosteric binding site, epibatidine moves more within this binding site, with only two binding events persisting until the end of the simulations (Figures S2E and F and S12). This higher mobility might explain why the observed Coulomb density cannot be clearly assigned to one specific molecule conformation. To ensure that binding is not an artifact of the periodic boundaries used during the simulations, we visually inspected the binding trajectories, verifying that epibatidine can reach the desensitization gate from the extracellular site (Figure S13). We further investigated epibatidine binding to the region of MB327-PAM-1, recently proposed for resensitizing ligands that allosterically modulate nAChR to counteract organophosphate poisoning.[18−21] However, in this region, only two unstable binding events were observed (Table S3). Noteworthy, we can also observe a high local correlation in the intracellular part of the nAChR (Figure 1A, Figure S9). However, the intracellular loop connecting the MA with the MX region is not resolved in the cryo-EM maps, which will potentially overlap with the suggested binding site (Figure S14).

Most interestingly, several PDB structures of nAChRs [$\alpha3\beta4$-nAChR (PDB IDs: 6PV7, 6PV8[22]), $\alpha4\beta2$-nAChR (PDB IDs: 5KXI[5], 6CNK, 6CNJ[23], 6UR8[24]), α7-nAChR (PDB ID: 7KOQ[4], 8F4V[25])] in the desensitized state have negatively charged glutamates at position −1′ pointing toward each other. For some of these structures (PDB IDs: 6PV7, 6PV8, 5KXI, &CNK, 6CNJ), it has been suggested that the negatively charged side chains are stabilized by a positively charged sodium ion.[5,22,23] Although sodium ions also bind in this region in our simulations of the active conformation, able to potentially stabilize negatively charged side chains in the desensitized state, we can also see clear occupancy density from other positively charged compounds such as TRIS and epibatidine (Figures S5, S8). This suggests that positively charged compounds may bind in this area with low selectivity, which might play a role in the activation−desensitization cycle of the receptor.

Our data collectively suggest that epibatidine, characterized as an orthosteric agonist of nAChRs, may also bind to the desensitization gate of α7-nAChR. Although these data are supported by the presence of significant Coulomb density in the cryo-EM map of the α7-nAChR that was not modeled, further experimental verification is required to corroborate this prediction and assess potential electrophysiological consequences. Estimation of the effective binding energy with MM-PBSA suggests that E237 and, to a lesser extent, S240 contribute toward epibatidine binding (Figure S15). To our knowledge, so far, only ligands that block the open channel but are located more to the extracellular side have been described.[26] As the desensitization gate is structurally highly similar between α7 and the other subtypes, including α_4, β_2, δ, ε, and γ, one can speculate that epibatidine can also bind to the desensitization gates. Minimizing a pose of epibatidine bound to the desensitization gate, generated by MD simulations of α7-nAChR in the active state, in the structure of the desensitized nAChR suggests that epibatidine might be present in the desensitization gate in the desensitized state of the nAChR (Figure S16). Mechanistically, the results enable one to speculate that epibatidine initially and likely more strongly binds to the orthosteric site, upon which the receptor is activated and the pore opens. Subsequently, epibatidine may also bind to the desensitization gate and stabilize the configuration of negatively charged glutamates, which may contribute to the complexity of α7-nAChR desensitization,[29] similar to what has been found for other desensitized structures.[4,5,22,23] More recent structures of α7-nAChR do not include unresolved densities at the desensitization gate. However, some, e.g., PDB ID: 7EKT[27], do not include epibatidine as a buffer component but rather encenicline, which is larger, and others, e.g., PDB ID: 8UT1[17], which do include epibatidine, possess a narrower diameter (by ∼3.3 Å in PDB ID: 8UT1) at the height of S240 compared to the structure of 7KOX. The prediction could be taken into account in the design of new ligands that modulate the activity of nAChRs and further our understanding of the activation−desensitization pathway of nAChRs.

■ ASSOCIATED CONTENT

Data Availability Statement

All study data are included in the article and/or Supporting Information. Files to recreate MD simulations, MD density and local correlation maps, and Pymol session files are provided in the supporting repository at https://doi.org/10.25838/d5p-81. For molecular simulations, the AMBER22 package of molecular simulation codes was used. AMBER22 is available from here: http://ambermd.org/.

Supporting Information

The Supporting Information is available free of charge at https://pubs.acs.org/doi/10.1021/acs.jcim.5c02384.

Additional materials and methods and figures and tables with results from MD simulations, as well as references (PDF)

■ AUTHOR INFORMATION

Corresponding Author

Holger Gohlke − *Institute for Pharmaceutical and Medicinal Chemistry, Heinrich Heine University Düsseldorf, 40225 Düsseldorf, Germany; Institute of Bio- and Geosciences (IBG-4: Bioinformatics), Forschungszentrum Jülich, Wilhelm-Johnen-Straße, 52425 Jülich, Germany;* orcid.org/0000-0001-8613-1447; Phone: (+49) 211 81 13662; Email: gohlke@hhu.de

Authors

Jesko Kaiser − *Institute for Pharmaceutical and Medicinal Chemistry, Heinrich Heine University Düsseldorf, 40225 Düsseldorf, Germany*

Christoph G. W. Gertzen − *Institute for Pharmaceutical and Medicinal Chemistry, Heinrich Heine University Düsseldorf,*

https://doi.org/10.1021/acs.jcim.5c02384
J. Chem. Inf. Model. 2026, 66, 1337−1341

40225 Düsseldorf, Germany; Center for Structural Studies (CSS), Heinrich Heine University Düsseldorf, 40225 Düsseldorf, Germany

Daniel Mann − *Ernst Ruska Centre (ER-C-3: Structural Biology), Forschungszentrum Jülich, Wilhelm-Johnen-Straße, 52425 Jülich, Germany;* orcid.org/0000-0002-9106-9358

Carsten Sachse − *Ernst Ruska Centre (ER-C-3: Structural Biology), Forschungszentrum Jülich, Wilhelm-Johnen-Straße, 52425 Jülich, Germany; Department of Biology, Heinrich Heine University, 40225 Düsseldorf, Germany*

Complete contact information is available at: https://pubs.acs.org/10.1021/acs.jcim.5c02384

Author Contributions

J.K.: Writing−original draft, Visualization, Investigation, Formal analysis. C.G.W.G.: Writing−review and editing, Visualization, Investigation, Formal analysis. D.M.: Writing−review and editing, Investigation, Formal analysis. C.S.: Writing−review and editing, Supervision, Formal analysis. H.G.: Writing−review and editing, Supervision, Project administration, Funding acquisition, Formal analysis, Conceptualization.

Funding

This work was supported by the German Ministry of Defense (E/U2AD/KA019/IF558). The Center for Structural Studies is funded by the DFG (Grant number 417919780).

Notes

The authors declare no competing financial interest.

■ ACKNOWLEDGMENTS

We are grateful for computational support and infrastructure provided by "Zentrum für Informations und Medientechnologie" (ZIM) at the Heinrich Heine University Düsseldorf and the computing time provided by the John von Neumann Institute for Computing (NIC) to HG on the supercomputer JUWELS at Jülich Supercomputing Center (JSC) (user IDs: VSK33, nAChR). The authors gratefully acknowledge the computing time granted by JARA Vergabegremium and provided on the JARA Partition part of the supercomputer JURECA at Forschungszentrum Jülich.[28]

■ REFERENCES

(1) Lee, C.-H.; Hung, S.-Y. Physiologic Functions and Therapeutic Applications of α7 Nicotinic Acetylcholine Receptor in Brain Disorders. *Pharmaceutics* **2023**, *15* (1), 31.

(2) Fatt, P. The electromotive action of acetylcholine at the motor end-plate. *J. Physiol* **1950**, *111* (3−4), 408−422.

(3) Katz, B.; Thesleff, S. A study of the desensitization produced by acetylcholine at the motor end-plate. *J. Physiol* **1957**, *138* (1), 63−80.

(4) Noviello, C. M.; Gharpure, A.; Mukhtasimova, N.; Cabuco, R.; Baxter, L.; Borek, D.; Sine, S. M.; Hibbs, R. E. Structure and gating mechanism of the α7 nicotinic acetylcholine receptor. *Cell* **2021**, *184* (8), 2121−2134.

(5) Morales-Perez, C. L.; Noviello, C. M.; Hibbs, R. E. X-ray structure of the human α4β2 nicotinic receptor. *Nature* **2016**, *538* (7625), 411−415.

(6) Turner, S. R.; Chad, J. E.; Price, M.; Timperley, C. M.; Bird, M.; Green, A. C.; Tattersall, J. E. Protection against nerve agent poisoning by a noncompetitive nicotinic antagonist. *Toxicol. Lett.* **2011**, *206* (1), 105−111.

(7) Seeger, T.; Eichhorn, M.; Lindner, M.; Niessen, K. V.; Tattersall, J. E.; Timperley, C. M.; Bird, M.; Green, A. C.; Thiermann, H.; Worek, F. Restoration of soman-blocked neuromuscular transmission in human and rat muscle by the bispyridinium non-oxime MB327 in vitro. *Toxicology* **2012**, *294* (2−3), 80−84.

(8) Niessen, K. V.; Seeger, T.; Rappengluck, S.; Wein, T.; Hofner, G.; Wanner, K. T.; Thiermann, H.; Worek, F. In vitro pharmacological characterization of the bispyridinium non-oxime compound MB327 and its 2- and 3-regioisomers. *Toxicol. Lett.* **2018**, *293*, 190−197.

(9) Scheffel, C.; Niessen, K. V.; Rappengluck, S.; Wanner, K. T.; Thiermann, H.; Worek, F.; Seeger, T. Electrophysiological investigation of the effect of structurally different bispyridinium non-oxime compounds on human alpha7-nicotinic acetylcholine receptor activity-An in vitro structure-activity analysis. *Toxicol. Lett.* **2018**, *293*, 157−166.

(10) Galzi, J. L.; Bertrand, S.; Corringer, P. J.; Changeux, J. P.; Bertrand, D. Identification of calcium binding sites that regulate potentiation of a neuronal nicotinic acetylcholine receptor. *Embo j* **1996**, *15* (21), 5824−5832.

(11) Hurst, R. S.; Hajós, M.; Raggenbass, M.; Wall, T. M.; Higdon, N. R.; Lawson, J. A.; Rutherford-Root, K. L.; Berkenpas, M. B.; Hoffmann, W. E.; Piotrowski, D. W.; et al. A novel positive allosteric modulator of the alpha7 neuronal nicotinic acetylcholine receptor: in vitro and in vivo characterization. *J. Neurosci.* **2005**, *25* (17), 4396−4405.

(12) Hedderich, J. B.; Persechino, M.; Becker, K.; Heydenreich, F. M.; Gutermuth, T.; Bouvier, M.; Bünemann, M.; Kolb, P. The pocketome of G-protein-coupled receptors reveals previously untargeted allosteric sites. *Nat. Commun.* **2022**, *13* (1), 2567.

(13) Kim, J. J.; Gharpure, A.; Teng, J.; Zhuang, Y.; Howard, R. J.; Zhu, S.; Noviello, C. M.; Walsh, R. M.; Lindahl, E.; Hibbs, R. E. Shared structural mechanisms of general anaesthetics and benzodiazepines. *Nature* **2020**, *585* (7824), 303−308.

(14) Masiulis, S.; Desai, R.; Uchański, T.; Serna Martin, I.; Laverty, D.; Karia, D.; Malinauskas, T.; Zivanov, J.; Pardon, E.; Kotecha, A.; et al. GABAA receptor signalling mechanisms revealed by structural pharmacology. *Nature* **2019**, *565* (7740), 454−459.

(15) Gohlke, H.; Hergert, U.; Meyer, T.; Mulnaes, D.; Grieshaber, M. K.; Smits, S. H. J.; Schmitt, L. Binding Region of Alanopine Dehydrogenase Predicted by Unbiased Molecular Dynamics Simulations of Ligand Diffusion. *J. Chem. Inf. Model.* **2013**, *53* (10), 2493−2498.

(16) Gopalswamy, M.; Kroeger, T.; Bickel, D.; Frieg, B.; Akter, S.; Schott-Verdugo, S.; Viegas, A.; Pauly, T.; Mayer, M.; Przibilla, J.; et al. Biophysical and pharmacokinetic characterization of a small-molecule inhibitor of RUNX1/ETO tetramerization with anti-leukemic effects. *Sci. Rep.* **2022**, *12* (1), 14158.

(17) Burke, S. M.; Avstrikova, M.; Noviello, C. M.; Mukhtasimova, N.; Changeux, J.-P.; Thakur, G. A.; Sine, S. M.; Cecchini, M.; Hibbs, R. E. Structural mechanisms of α7 nicotinic receptor allosteric modulation and activation. *Cell* **2024**, *187* (5), 1160−1176.

(18) Kaiser, J.; Gertzen, C. G. W.; Bernauer, T.; Höfner, G.; Niessen, K. V.; Seeger, T.; Paintner, F. F.; Wanner, K. T.; Worek, F.; Thiermann, H.; et al. A novel binding site in the nicotinic acetylcholine receptor for MB327 can explain its allosteric modulation relevant for organophosphorus-poisoning treatment. *Toxicol. Lett.* **2023**, *373*, 160−171.

(19) Nitsche, V.; Höfner, G.; Kaiser, J.; Gertzen, C. G. W.; Seeger, T.; Niessen, K. V.; Steinritz, D.; Worek, F.; Gohlke, H.; Paintner, F. F.; et al. MS Binding Assays with UNC0642 as reporter ligand for the MB327 binding site of the nicotinic acetylcholine receptor. *Toxicol. Lett.* **2024**, *392*, 94−106.

(20) Bernauer, T.; Nitsche, V.; Kaiser, J.; Gertzen, C. G. W.; Höfner, G.; Niessen, K. V.; Seeger, T.; Steinritz, D.; Worek, F.; Gohlke, H.; et al. Synthesis and biological evaluation of novel MB327 analogs as resensitizers for desensitized nicotinic acetylcholine receptors after intoxication with nerve agents. *Toxicol. Lett.* **2024**, *397*, 151−162.

(21) Kaiser, J.; Gertzen, C. G. W.; Bernauer, T.; Nitsche, V.; Höfner, G.; Niessen, K. V.; Seeger, T.; Paintner, F. F.; Wanner, K. T.; Steinritz, D.; et al. Identification of ligands binding to MB327-PAM-1,

a binding pocket relevant for resensitization of nAChRs. *Toxicol. Lett.* **2024**, *398*, 91.
(22) Gharpure, A.; Teng, J.; Zhuang, Y.; Noviello, C. M.; Walsh, R. M.; Cabuco, R.; Howard, R. J.; Zaveri, N. T.; Lindahl, E.; Hibbs, R. E. Agonist Selectivity and Ion Permeation in the $\alpha 3\beta 4$ Ganglionic Nicotinic Receptor. *Neuron* **2019**, *104* (3), 501−511.
(23) Walsh, R. M.; Roh, S.-H.; Gharpure, A.; Morales-Perez, C. L.; Teng, J.; Hibbs, R. E. Structural principles of distinct assemblies of the human $\alpha 4\beta 2$ nicotinic receptor. *Nature* **2018**, *557* (7704), 261−265.
(24) Mukherjee, S.; Erramilli, S. K.; Ammirati, M.; Alvarez, F. J. D.; Fennell, K. F.; Purdy, M. D.; Skrobek, B. M.; Radziwon, K.; Coukos, J.; Kang, Y.; et al. Synthetic antibodies against BRIL as universal fiducial marks for single−particle cryoEM structure determination of membrane proteins. *Nat. Commun.* **2020**, *11* (1), 1598.
(25) Bondarenko, V.; Chen, Q.; Singewald, K.; Haloi, N.; Tillman, T. S.; Howard, R. J.; Lindahl, E.; Xu, Y.; Tang, P. Structural Elucidation of Ivermectin Binding to $\alpha 7$nAChR and the Induced Channel Desensitization. *ACS Chem. Neurosci.* **2023**, *14* (6), 1156−1165.
(26) Haufe, Y.; Loser, D.; Danker, T.; Nicke, A. Symmetrical Bispyridinium Compounds Act as Open Channel Blockers of Cation-Selective Ion Channels. *ACS Pharmacology & Translational Science* **2024**, *7* (3), 771−786.
(27) Zhao, Y.; Liu, S.; Zhou, Y.; Zhang, M.; Chen, H.; Eric Xu, H.; Sun, D.; Liu, L.; Tian, C. Structural basis of human $\alpha 7$ nicotinic acetylcholine receptor activation. *Cell research* **2021**, *31* (6), 713−716.
(28) Thornig, P. JURECA: Data Centric and Booster Modules implementing the Modular Supercomputing Architecture at Jülich Supercomputing Centre. *Journal of Large-Scale Research Facilities* **2021**, *7*, A182−A182.
(29) Avstrikova, M.; Milan Rodriguez, P.; Burke, S. M.; Hibbs, R. E.; Changeux, J.-P.; Cecchini, M. Hidden complexity of $\alpha 7$ nicotinic acetylcholine receptor desensitization revealed by MD simulations and Markov state modeling. *Proc. Natl. Acad. Sci. U. S. A.* **2025**, *122*, No. e2420993122.

https://doi.org/10.1021/acs.jcim.5c02384
J. Chem. Inf. Model. 2026, 66, 1337−1341